

# Profile of cryptobrachytone C accumulation in *Cryptocarya pulchrinervia* leaves using MALDI-MSI

JUJUN RATNASARI<sup>1,♥</sup>, RIZKITA RACHMI ESYANTI<sup>1</sup>, MARSELINA IRASONIA TAN<sup>2</sup>,  
LIA DEWI JULIAWATY<sup>3,♥♥</sup>, SHUICHI SHIMMA<sup>4,♥♥♥</sup>

<sup>1</sup>Plant Sciences and Biotechnology Laboratory, School of Life Sciences and Technology, Institut Teknologi Bandung. Jl. Ganesa 10, Bandung 40132, West Java, Indonesia. Tel.: +62-22-2511575, ♥email: jujun.ratnasari@gmail.com

<sup>2</sup>Animal Physiology, Developmental Biology and Biomedical Sciences Laboratory, School of Life Sciences and Technology, Institut Teknologi Bandung. Jl. Ganesa 10, Bandung 40132, West Java, Indonesia

<sup>3</sup>Organic Chemistry Laboratory, Chemistry Program, Faculty of Mathematics and Natural Sciences, Institut Teknologi Bandung. Jl. Ganesa 10, Bandung 40132, West Java, Indonesia. Tel.: +62-22-2515032, ♥♥email: liadewi@chem.itb.ac.id

<sup>4</sup>Department of Biotechnology, Graduate School of Engineering, Osaka University. 2-1 Yamadaoka, Suita, Osaka, 565-0871, Japan. ♥♥♥email: sshimma@bio.eng.osaka-u.ac.jp

Manuscript received: 22 December 2020. Revision accepted: 6 February 2021.

**Abstract.** Ratnasari J, Esyanti RR, Tan MI, Juliawaty LD, Shimma S. 2021. Profile of cryptobrachytone C accumulation in *Cryptocarya pulchrinervia* leaves using MALDI-MSI. *Biodiversitas* 22: 1172-1178. Cryptobrachytone C is an active compound isolated from leaves of *Cryptocarya pulchrinervia*, an indigenous plant from Indonesia. Cryptobrachytone C is cytotoxic against P388 leukemia cancer cell lines. A profile of cryptobrachytone C accumulation in leaves based on physiological age is necessary to study cryptobrachytone C production in the plant since it has anticancer potential. *In situ* profiling of cryptobrachytone C accumulation in leaves was carried out by imaging techniques using matrix-assisted laser desorption/ionization mass spectrometry imaging (MALDI-MSI). The cryptobrachytone C ionization efficiency was carried out by derivatization using Girard-T reagent and coating with  $\alpha$ -cyano-4-hydroxycinnamic acid ( $\alpha$ -CHCA) matrix. Scanned leaves show higher accumulation intensity in the second leaf. Quantitative accumulation profiling was conducted using GC-MS, where the highest amount of cryptobrachytone C was on the second leaf at  $87.07 \pm 47.21$  mg. This showed that the most effective isolation of cryptobrachytone C would be obtained from young leaves of *Cryptocarya pulchrinervia*. This profile would play a role in cryptobrachytone C production *in-situ* or *ex-situ* using tissue culture.

**Keywords:** *Cryptocarya pulchrinervia*, cryptobrachytone C, MALDI-MSI, mass spectrometry.

**Abbreviations:** MALDI-MSI: matrix-assisted laser desorption/ionization mass spectrometry imaging;  $\alpha$ -CHCA:  $\alpha$ -cyano-4-hydroxycinnamic acid; GC-MS: gas chromatography-mass spectrometer; GT: Girard's reagent T; ITO: indium-tin-oxide

## INTRODUCTION

Plants are autotrophic organisms that play a crucial role in life on earth. They could form organic compounds from inorganic compounds through photosynthesis. These organic compounds, especially secondary metabolites, play a role in plant defense against pests, disease, and environmental stressors. Communities generally use plants' secondary metabolites as food, clothing, industrial raw materials, and medicine. Plant's secondary metabolites that have bioactivities are used as antibacterial, anticancer, antifungal, and antiviral medicine, and they are used for the development of novel drug substances as well as for cosmetics (Gechev et al. 2014; Kaur et al. 2011; Raina et al. 2014). Traditionally they were used as a drug because they were easy to use and inexpensive (Shah et al. 2013). Many anticancer drugs that are used today come from a plant's secondary metabolites (Cragg and Newman 2005).

Some plant's secondary metabolites are used as anticancer drugs, for example, vincristine and vinblastine

isolated from *Catharanthus roseus*, colchicine isolated from *Colchicum autumnal*, taxol and paclitaxel isolated from *Taxus brevifolia*, andrographol isolated from *Andrographis paniculata*, morindron isolated from *Morinda citrifolia* (Cragg and Newman 2005; Raina et al. 2014), acetogenin from *Annona muricata*, and mangosteen from *Garcinia mangostana* (Amin et al. 2009). Many plants that produce secondary metabolites that have potential as anticancer drugs belong to the Lauraceae family. Lauraceae is a family of higher plants with a distinctive character. There are aromatic compounds in the leaves and bark (Kostermans 1957). Several genera of Lauraceae have potential anticancer compounds. One of them is the genus *Cryptocarya* (Table 1) (Juliawaty et al. 2006). *Cryptocarya pulchrinervia* is an indigenous Indonesian plant. It has a compound that is cytotoxic against leukemia cancer cell lines P388 (Juliawaty et al. 2020), namely CP-2, which has good potential to be developed as an anticancer drug.

**Table 1.** Antiproliferative compounds from the genus *Cryptocarya*

Compound	Class	Species	Cell line	Ref.
Cryptomoscatone D2	Pyron	<i>C. mandioccana</i>	HeLa, SiHa, C33A	Giocondo et al. 2009
Cryptocaryone (CPC)		<i>C. concinna</i>	Ca9-22, CAL 27	Chang et al. 2016
Rugulacton		<i>C. rugulosa</i>	MCF-7, MDA-MB-231	Mohapatra et al. 2014
Anthofine and Dehydroanthofine	Alkaloid	<i>C. chinensis</i>	L-1210, P-388, A-549, HCT-8	Wu et al. 2012

This compound was isolated from the leaves of *Cryptocarya pulchrinervia* and is classified as a pyron compound (Juliawaty et al. 2020). The same compound has already been published. It was isolated from an indigenous Chinese *Cryptocarya brachityrsa* and was named cryptobrachytone C (Fan et al. 2019). CP-2, then, is referring to cryptobrachytone C. The accumulation profile of this compound in leaves has not yet been studied. Information on the accumulation of compounds on leaves based on physiological age is crucial information, given that each secondary metabolite compound in plants has a synthesis site and an accumulation site that can be the same or different depending on metabolism, physiological activity, and developmental stage (Puzanskiya et al. 2018; Sturtevant et al. 2016). The synthesis and accumulation of site information are crucial to determine the best sample for isolation. This information is also overriding to the development of the production of these compounds as potential anticancer drugs.

Profiling the accumulation of secondary metabolites in plants could be done both *in-situ* and *ex-situ* (Dong et al. 2016). *In-situ* profiling could be done through direct compound scanning on tissues or organs using matrix-assisted laser desorption/ionization-mass spectrometry imaging (MALDI-MSI) (Muller et al. 2011; Sturtevant et al. 2016). *Ex-situ* profiling could be done using extraction methods then measuring the quality and quantity using GC-MS or LC-MS. The MALDI-MSI technique could produce images of the localization of molecules in the tissue through ionization and direct detection (Qin et al. 2018). Qualitative assessment of compound concentrations is based on the color of the image and the relative intensity that appears on the spectrum.

## MATERIALS AND METHODS

In testing samples using MALDI-MSI, the matrix played a crucial role in absorbing UV energy or laser irradiation. It could absorb and ionize analytes on the matrix and specimens optimally. To determine the type of matrix to be used, the  $m/z$  of a standard compound was measured. Various kinds of matrices are used to measure the  $m/z$  of a standard and the spectrum peak desired analyte. If the spectrum is visible, the matrix would be used for the next measurements. If the compound was not well ionized and detected, it was necessary to optimize the ionization using on-tissue chemical derivatization (OTCD). OTCD can be used as a tool to study the spatial distribution of poorly ionizable molecules within tissue (Claes et al. 2019; Harkin et al. 2021). Derivatization was carried out in

this study using Girard's reagent T (GT) (Shimma et al. 2016).

### Sample preparation for MALDI-MSI

Fresh leaves of *Cryptocarya pulchrinervia* were obtained from the Bogor Botanical Gardens, Indonesia. The samples were wrapped in air-tight plastic and placed at a temperature of 4°C. Preparation of the leaf samples was initiated by scraping the abaxial cuticle of the leaves. Then, the leaves were cut into shape to fit in the objective glass. The adaxial side of the leaves was affixed to the conductive indium-tin-oxide (ITO) glass. The affixing used conductive double-sided tape. The abaxial side of the leaves was exposed to the derivatization and matrix application. The finished preparations were then placed into a tube containing silica gel and stored at a temperature of 4°C. Before the matrix and derivatization application, samples were captured with the MALDI-MSI instrument (iMscope TRIO Shimadzu) to take the original pictures.

### Derivatization

The ITO glass with the samples was clamped with a holder and inserted into MALDI-MSI. The image to be taken before the matrix applies to the sample. After being photographed, the preparation was removed for cryptobrachytone C derivatization using GT reagent (GT, 10 mg/ml in 20% acetic acid). GT derivatization using by manual spraying it over the sample using an artist airbrush (PS-270, GSI Creos, Tokyo, Japan). The preparation was performed and kept at room temperature for 60 minutes.

### MALDI-MSI matrix application

Matrix applications were performed using two methods, namely vacuum sublimation and spraying. Sublimation used iMLayer (Shimadzu, Kyoto, Japan) with  $\alpha$ -cyano-4-hydroxycinnamic acid ( $\alpha$ -CHCA) matrix (Merck, Darmstadt, Germany), while spraying used an artist's airbrush (PS-270, GSI Creos, Tokyo, Japan) with the same matrix. The sample was sprayed at a distance of 8 cm from the tip of the airbrush to the sample surface. After applying the matrix, the preparation was dried at room temperature, then tested with the MALDI-MSI instrument (iMscope TRIO, Shimadzu, Kyoto Japan) equipped with an Nd:YAG laser ( $\lambda = 355$  nm). The laser spot size was set at approximately 12.5  $\mu$ m. The mass resolution was 15,000 (full width at half maximum) at  $m/z$  200. The ion images and the spectra were obtained using tandem mass spectrometry (MS/MS) mode. The obtained data was then analyzed with the Imaging MS solution (Shimadzu, Kyoto, Japan).

### Sample extraction for GC-MS

The leaves of *C.pulchrinervia* were dried and macerated in acetone for 3 x 24 hours. The macerate was then dissolved in methanol-water in a ratio of 1:1 and extracted with ethyl acetate to separate chlorophyll. Ethyl acetate extract then fractionated using vacuum liquid chromatography with *n*-hexane-ethyl acetate as eluent in a ratio of 7: 3. Each fraction was dry with a rotary evaporator. Furthermore, separation of the fraction using chromatography of gravity columns. Once the fraction containing the most cryptobrachytone C and the least impurities, purification was carried out using the crystallization method.

### GC-MS

GC-MS was used to measure cryptobrachytone C concentration quantitatively in triplicate. Leaf extract was dissolved in ethyl acetate and measured using GC-MS (6890 GC) with Agilent column 19091S-433 HP-5MS 5% phenyl methyl siloxane at a temperature of 325°C, with a speed of 36 cm/sec. Willey09th was used for identification for GC-MS analysis. Cryptobrachytone C crystal was used as external standard dissolved in ethyl acetate.

## RESULTS AND DISCUSSION

### Cryptobrachytone C derivatization with Girard T (GT)

In the standard sample testing using the  $\alpha$ -CHCA matrix, it was found that protonated peak derived from cryptobrachytone C had  $m/z$  289.14. When measured with MALDI-MSI on the leaf surface, the peak in the obtained spectrum was not sharp and did not separated from the chemical noise (Figure 1). This was caused by the ionization suppression of cryptobrachytone C due to impure samples. To improve the ionization efficiency, GT was used for derivatization. GT could easily be ionized by the laser because it has trimethylamine with a positive charge (Shimma, 2016). GT would bind with cryptobrachytone C in the ketone group in the aliphatic chain (Figure 2.A).

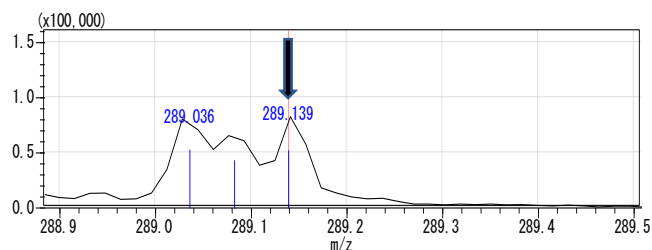
Furthermore, in the GT-C cryptobrachytone compound, MS/MS was performed to release the trimethylamine so that compounds with  $m/z$  of 343.17 were detected (Figure 2.B) using the  $\alpha$ -CHCA matrix.

### Spectrum of cryptobrachytone C in leaves of *Cryptocarya pulchrinervia*

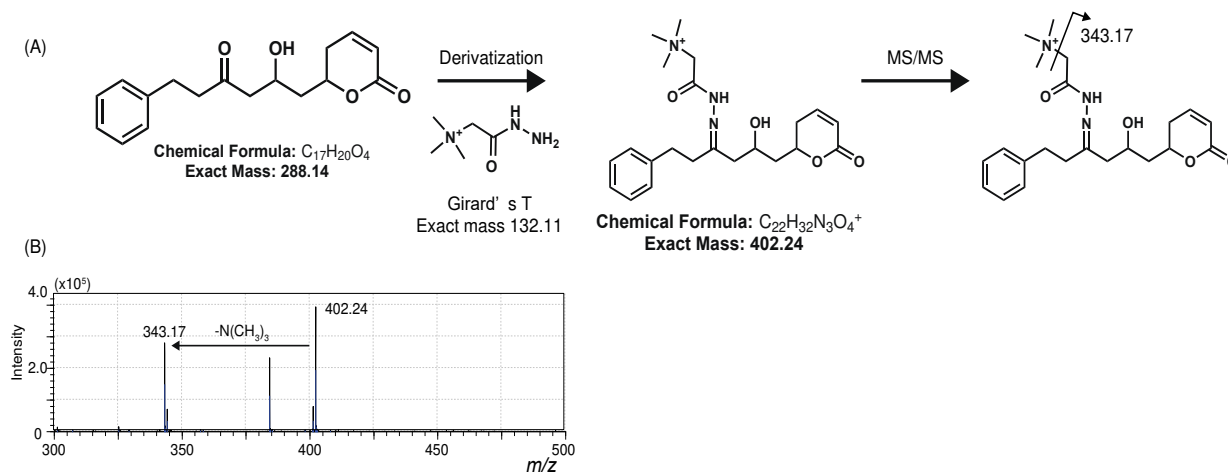
Imaging results showed that cryptobrachytone C was distributed throughout the leaf, from the first leaf to the fifth leaf. This was indicated by the intensity of the color of the compounds seen in the spectrum. The spectrum showed that red indicated the highest relative intensity of cryptobrachytone C, and blue indicated the lowest relative intensity. The obtained spectrum was then overlaid with an image of the sample that had not been treated with GT or the matrix so as to obtain a picture of the relative intensity of cryptobrachytone C in the leaf tissue (Figure 3).

### GC-MS analysis result

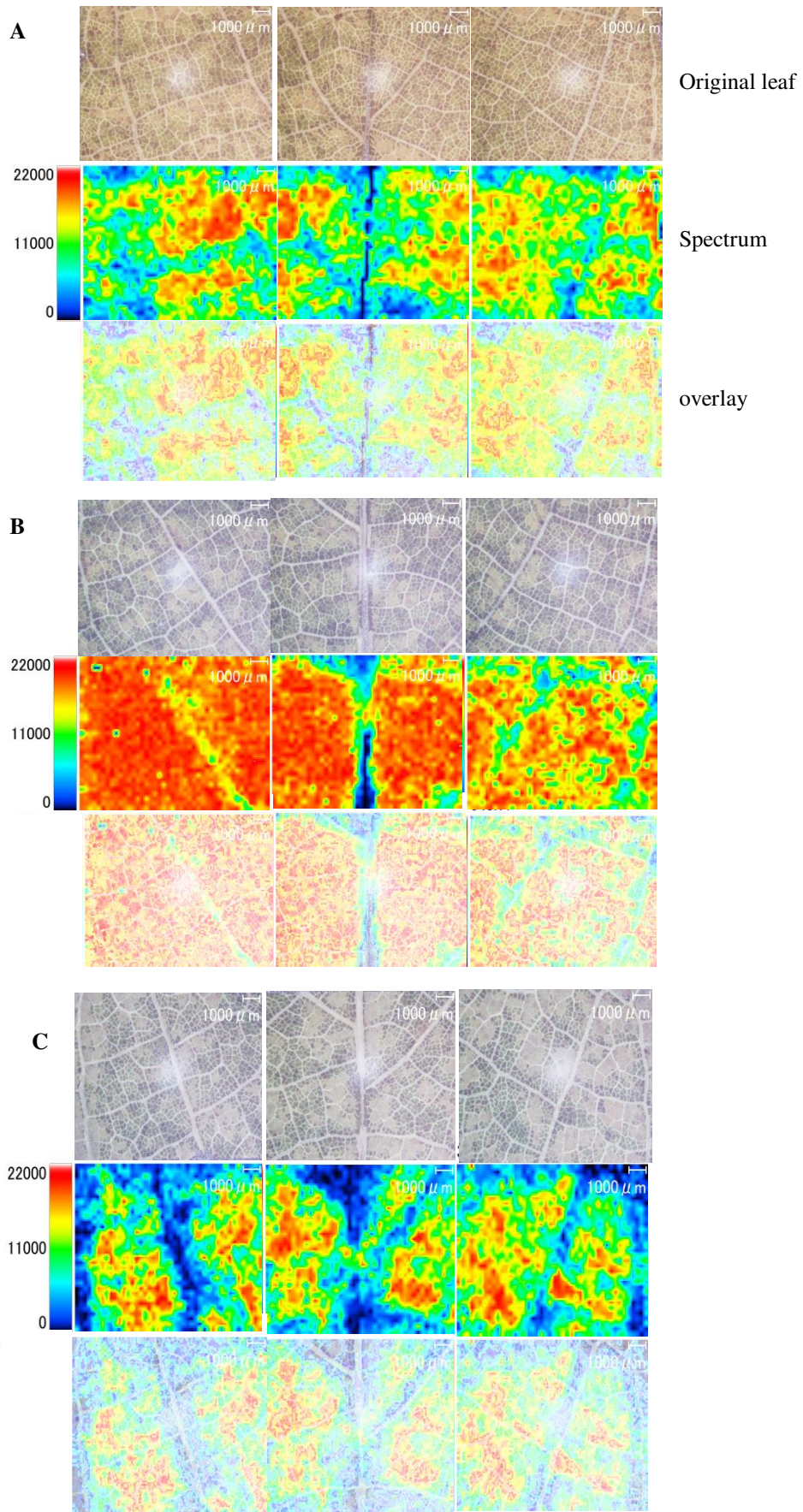
Qualitatively, the spectrum showed that accumulation of cryptobrachytone C was present in all leaves (Figure 3), with the highest relative intensity in the second leaf, followed by the first, third, fourth, and fifth leaves. Similarly, the quantitative test results using GC MS (Figure 4). The highest cryptobrachytone C accumulation was in the young leaves (Figure 5).



**Figure 1.** The enlarged mass spectrum around  $m/z$  289.14 derived from the native Cryptobrachytone C ( $[M+H]^+$ ). The detected peak was not separated from the chemical noise



**Figure 2.** Derivatization of cryptobrachytone C. (A) Schematic drawing of derivatization with Girard's T reagent (GT) (B) product ion spectrum of derivatized cryptobrachytone C. In the spectrum, expected product ion peak at  $m/z$  343.17 was detected



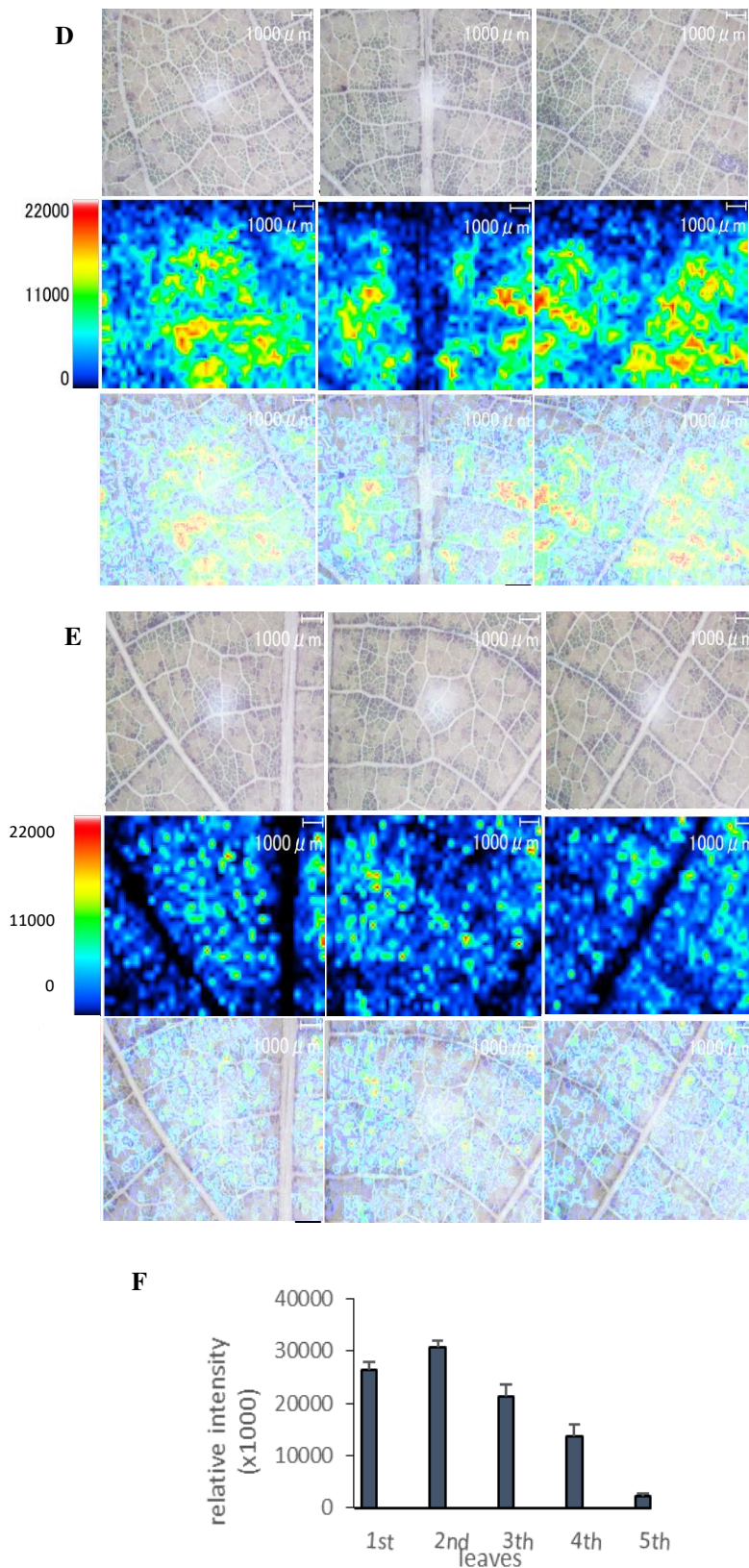


**Figure 3.** The spectrum of cryptobrachytone C from the first to the fifth leaf (A-E) analyze in triplicated. The higher relative intensity of cryptobrachytone C on mesophyll showed in red color, while the blue color showed the lowest relative intensities. The original image show leaves before the treatment of both of  $\alpha$ -CHCA matrix nor GT. The relative intensities of cryptobrachytone C at 22  $\mu\text{m}$  pixel size. The accumulation of the cryptobrachytone C is on the mesophyll instead of on the vascular tissue. And the relative intensities of the second leaves were higher than other leaves ( $p=0.059$ ) (F)

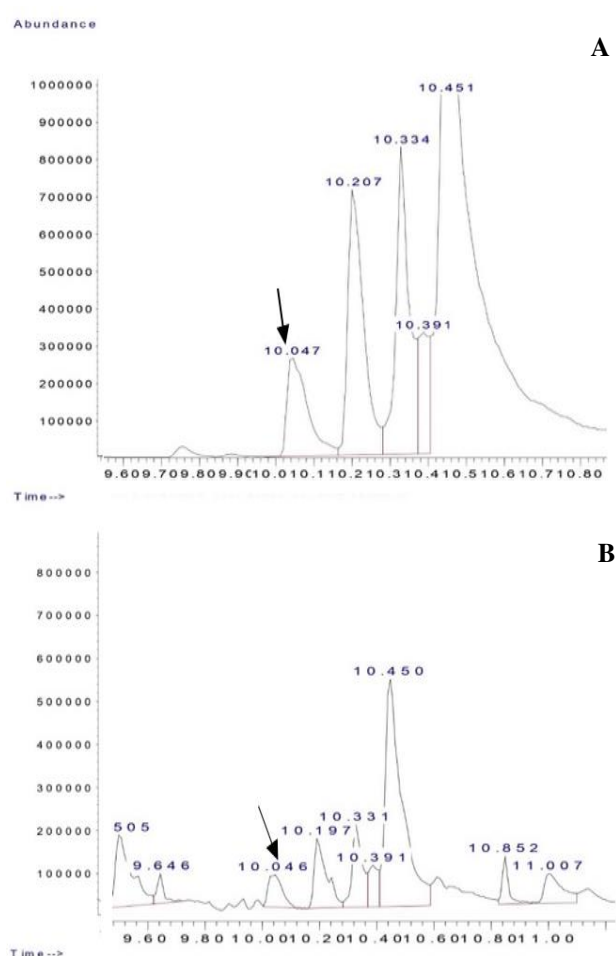


**Figure 4.** Cryptobrachytone C standard spectrum by GC MS showed retention time in 10.047 (A). The lowest amount of cryptobrachytone C in the 5th leaf sample showed in chromatogram with a retention time of 10.046 (B).

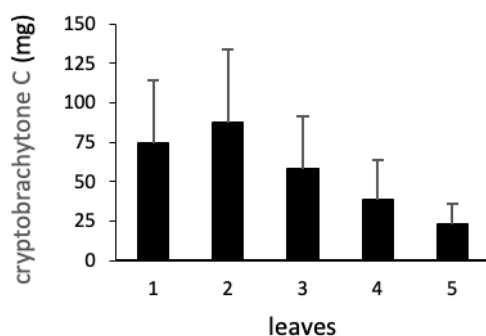


**Figure 5.** Cryptobrachytone C on leaves of *Cryptocarya pulchrinervia* is highest in the second leaf than in the first leaf. Assuming that the compound synthesis is in the young leaves instead of in old leaves.

## Discussion

Accumulation of cryptobrachytone C on the leaves of *Cryptocarya pulchrinervia* was examined in-situ

using mass spectrometry MALDI-MSI. MALDI-MSI can determine the distribution of biological molecules that can be ionized in whole organs and at incision preparations (Qin et al. 2018). The leaf preparation involved scraping the cuticle due to the leaves being dry and rigid. The leaves could not be sliced manually nor by a microtome. The cuticle is the main obstacle that could inhibit the matrix to extract the compound since the cuticle has wax layers. A sample sliced by microtome is a lot easier to ionize by the matrix. Scraping off the *Cryptocarya pulchrinervia* leaves could not get rid of all the cuticles, so the wax layer remained and became a barrier to the matrix to optimally extract cryptobrachytone C. The ionization of cryptobrachytone C could be increased with derivatization using GT compound (Shimma 2016). The presence of trimethylamine in the GT compound can increase the positive charge on the cryptobrachytone bonds with the GT, increasing the sensitivity to detection by MS. So, cryptobrachytone C would ionize to the maximum (Zhang et al. 2019). Derivatization and MS/MS technique showed that cryptobrachytone C could be extracted by  $\alpha$ -CHCA optimally in  $m/z$  343.17. The relative intensity of cryptobrachytone C showed on the spectrum with a different color. The blue color showed low relative intensities, and the red color showed high relative intensities.

The site of cryptobrachytone C accumulation can be observed by overlaying the original image with the spectrum. Cryptobrachytone C on the leaves was detected in the mesophyll but not in the vessel tissue. This would be caused by a vessel's function only as a compound transportation tool, not as an accumulation site. In the higher plant, the metabolites will be distributed to other places by fascicular vessel and extravascular tissue in symplast and apoplast mode (Boughthon et al. 2016). The highest accumulation is in the young leaves, so it could be estimated that the cryptobrachytone C synthesis occurs in the young leaves. This is due to the leaves function where the biological processes of plants occur, such as photosynthesis, environmental stress sensors, and plant defense (Qin et al. 2018). In the higher plant, synthesis and accumulation of secondary metabolite were generally dependent on the physiological activity and the developmental stage of plants (Puzanskiya et al. 2018).

Cryptobrachytone C accumulated in the first to fifth leaves of *Cryptocarya pulchrinervia* based on their physiological age. Higher accumulation of cryptobrachytone C in young leaves could be caused by a different stage of the plant's development, or could be caused by physiological conditions, such as the sensitivity of young leaves to internal and external stressors being higher compared to older leaves (González-Villagra et al. 2018). Increased sensitivity to stressors would trigger the synthesis of the secondary metabolites that play a role in the plant's defense system (Puzanskiya et al. 2018). The profile of cryptobrachytone C accumulation between the first and second leaves was similar in intensity and amount due to similar physiological age as young leaves. As for the third, fourth, and fifth leaves, the relative intensities and amount are less because of the older the physiological age,

the less sensitivity to stressors (González-Villagra et al. 2018). Cryptobrachytone C profile on the leaves of *Cryptocarya pulchrinervia* would contribute to the optimization of sample selection extraction. This could also be the basis for the development of production *in vitro* given that the potential of cryptobrachytone C as a drug is high because it has high cytotoxic activities.

## ACKNOWLEDGEMENTS

This research fund by the WCU ITB sandwich program and the BUDI-DN scholarship program of the Directorate General of Higher Education and the Ministry of Finance's Educational Fund Management Agency, Republic of Indonesia. Thank you very much to the Bogor Botanical Gardens, Indonesia that provided samples of *Cryptocarya pulchrinervia* leaves.

## REFERENCES

- Amin A, Muhtasib HG, Ocker M, Stock RS. 2009. Overview of major classes of plant-derived anticancer drugs. *Int J Biomed Sci* 5 (1): 1-11.
- Boughton BA, Thinagaran D, Sarabia D, Bacic A, Roessner U. 2016. Mass spectrometry imaging for plant biology: A review. *Phytochem Rev* 15 (3): 445-488. DOI: 10.1007/s11101-015-9440-2
- Chang HS, Tang JY, Yen CY, Huang HW, Wu CY, Chung YA, Wang HR, Chen IS, Huang MY, Chang HW. 2016. Antiproliferation of *Cryptocarya concinna* derived cryptocaryone against oral cancer cells involving apoptosis, oxidative stress, and DNA damage. *BMC Complement Altern Med* 16: 94. DOI: 10.1186/s12906-016-1073-5
- Claes BS, Takeo E, Fukusaki E, Shimma S, Heeren RM. 2019. Imaging isomers on a biological surface: A review. *Mass Spectrometry* 8 (1): A0078-A0078.
- Cragg GM, Newman DJ. 2005. Plants as a source of anti-cancer agents. *J Ethnopharmacol* 100 (1-2): 72-79. DOI: 10.1016/j.jep.2005.05.011
- Dong Y, Li B, Malitzky S, Rogachev I, Aharoni A, Kaftan F, Svatos A, Franceschi P. 2016. Sample preparation for mass spectrometry imaging of plant tissues: A review. *Front Plant Sci* 7: 60. DOI: 10.3389/fpls.2016.00060
- Fan Y, Liu Y, You YX, Rao L, Su Y, He Q, Hu F, Li Y, Wei W, Xu YK, Lin B, Zhang CR. 2019. Cytotoxic arylalkenyl  $\alpha$ ,  $\beta$ -unsaturated  $\delta$ -lactones from *Cryptocarya brachythyrsa*. *Fitoterapia* 136: 104167. DOI: 10.1016/j.fitote.2019.05.006
- Gechev TS, Hille J, Woerdenbag HJ, Benina M, Mehterov N, Toneva V, Fernie AR, Bernd Mueller-Roeber, Mueller-Roeber B. 2014. Natural products from resurrection plants: Potential for medical applications. *Biotechnol Adv* 32 (6): 1091-1101. DOI: 10.1016/j.biotechadv.2014.03.005.
- Giocondo MP, Bassi CL, Telascra M, Cavalheiro AJ, Bolzani VS, Silva DHS, Agustoni D, Mello ER, Soares CP. 2009. Kriptomoskatone d2 from *Cryptocarya mandiocana*: Cytotoxicity against human cervical carcinoma cell line. *Revista de Ciencias Farmaceuticas Basica e Aplicada* 30 (3): 315-322.
- González-Villagra J, Rodrigues-Salvador A, Nunes-Nesi A, Cohen JD, Reyes-Díaz MM. 2018. Age-related mechanism and its relationship with secondary metabolism and abscisic acid in *Aristotelia chilensis* plants subjected to drought stress. *Plant Physiol Biochem* 124: 136-145. DOI: 10.1016/j.plaphy.2018.01.010.
- Harkin C, Smith KW, Cruickshank FL, Logan Mackay C, Flinders B, Heeren RM, Moore T, Brockbank S, Cobice DF. 2021. On-tissue chemical derivatization in mass spectrometry imaging. *Mass Spectrometry Rev*. DOI: 10.1002/mas.21680.
- Juliawaty LD, Aimi N, Ghisalberti EL, Katajima M, Makmur L, Syah YM, Siallagan J, Tahayaka K, Achmad SA, Hakim EH. 2006. Chemistry of Indonesian *Cryptocarya* plants (Lauraceae). In: Brahmachari G. (ed.), *Chemistry of Natural Products, Recent Trends & Developments*. 2 ed. Research Signpost, Trivandrum, India.
- Juliawaty LD, Ra'idah PN, Abdurrahman S, Hermawati E, Alni A, Tan MI, Ishikawa H, Syah YM. 2020. 5, 6-Dihydro- $\alpha$ -pyrones from the leaves of *Cryptocarya pulchrinervia* (Lauraceae). *J Nat Med* 74: 584-590. DOI: 10.1007/s11418-020-01397-7.
- Kaur R, Kapoor K, Kaur H. 2011. Plants as a source of anticancer agents. *J Nat Prod Plant Resour* 1 (1): 119-124.
- Kostermans AJGH. 1957. *Reinwardtia*. *Herbarium-Bogoriense*. *Kebun Raya Indonesia* 4 (2): 193-256.
- Mohapatra DK, Reddy DS, Ramaiah MJ, Ghosh S, Pothula V, Lunavath S, Thomas S, Valli SNCVLP, Pal Bhadra M, Yadav JS. 2014. Rugulactone derivatives act as inhibitors of NF- $\kappa$ B activation and modulates the transcription of NF- $\kappa$ B dependent genes in MDA-MB-231 cells. *Bioorg Med Chem Lett* 24 (5): 1389-1396. DOI: 10.1016/j.bmcl.2014.01.030.
- Muller T, Oradu S, Ifa DR, Cooks RG. 2011. Direct plant tissue analysis and imprint imaging by desorption electrospray ionization mass spectrometry. *Am Chem Soc* 83: 5754-5761.
- Puzanskiya RK, Yemelyanova VV, Shavardaa ALC, Gavrilenko TA, Shishovaa MF. 2018. Age and organ-specific differences of potato (*Solanum phureja*) plants metabolome. *Russian J Plant Physiol* 65: 813-823. DOI: 10.1134/S1021443718060122.
- Qin L, Zhang Y, Liu Y, He H, Han M, Li Y, Zeng M, Wang X. 2018. Recent advances in matrix-assisted laser desorption/ionization mass spectrometry imaging (MALDI-MSI) for in situ analysis of endogenous molecules in plants. *Phytochem Anal* 29: 351-364. DOI: 10.1002/pca.2759.
- Raina H, Soni G, Jauhari N, Sharma N, Bharadvaja N. 2014. Phytochemical importance of medicinal plants as potential sources of anticancer agents. *Himani Turk J Bot* 38: 1027-1035.
- Shah U, Shah, R Acharya S, Acharya N. 2013. Novel anticancer agents from plants sources. *Chinese J Nat Med* 11 (1): 16-23. DOI: 10.1016/S1875-5364(13)60002-3.
- Shimma S, Kumada HO, Taniguchi H, Konno A, Yao I, Furuta K, Matsuda T, Ito S. 2016. Microscopic visualization of testosterone in mouse testis by use of imaging mass spectrometry. *Anal Bioanal Chem* 408 (27): 7607-7615. DOI: 10.1007/s00216-016-9594-9.
- Sturtevant D, Lee YJ, Chapman KD. 2016. Matrix-assisted laser desorption/ionization-mass spectrometry imaging (MALDI-MSI) for direct visualization of plant metabolites in situ. *Plant Biotechnol* 37: 53-60. DOI: 10.1016/j.copbio.2015.10.004.
- Wu TS, Sua CR, Lee KH. 2012. Cytotoxic and anti-HIV phenanthroindolizidine alkaloids from *Cryptocarya chinensis*. *Nat Prod Commun* 7 (6): 725-727.
- Zhang Y, Wang B, Jin W, Wen Y, Nan L, Yang M, Song X. 2019. Sensitive and robust MALDI-TOF-MS glycomics analysis enabled by Girard's reagent T on-target derivatization (GTOD) of reducing glycans. *Analytica Chimica Acta* 1048: 105-114. DOI: 10.1016/j.aca.2018.10.015.